

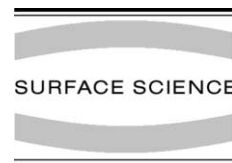


ELSEVIER

Available online at [www.sciencedirect.com](http://www.sciencedirect.com)

SCIENCE @ DIRECT®

Surface Science 523 (2003) 241–251

[www.elsevier.com/locate/susc](http://www.elsevier.com/locate/susc)

# Molecular and dissociative bonding of amines with the Si(1 1 1)-(7 × 7) surface

Xiaoping Cao, Robert J. Hamers \*

*Department of Chemistry, University of Wisconsin-Madison, 1101 University Avenue, Madison, WI 53706, USA*

Received 25 January 2002; accepted for publication 7 June 2002

## Abstract

The interaction of trimethylamine (TMA) and dimethylamine (DMA) with the Si(1 1 1)-(7 × 7) surface has been studied by scanning tunneling microscopy (STM), X-ray photoelectron spectroscopy (XPS), and ultraviolet photoemission spectroscopy (UPS). STM data for TMA at low coverage show molecular features exhibiting a strong preference for bonding at the center adatom sites. XPS data show that at low coverage the majority of molecules form a highly ionic dative-bonded molecular adduct in which the N atom donates electron density to the surface, leading to a very high N(1s) binding energy of 402.4 eV. UPS data show that the interaction of TMA with the Si(1 1 1)-(7 × 7) surface also involves the restatom, suggesting that formation of dative bonds may also alter the restatom state. At very high exposures, a new, dissociative pathway becomes important, leading to dissociation and the appearance of new fragments with lower N(1s) binding energies of 399.1 eV. Corresponding studies for DMA only show dissociative bonding on Si(1 1 1), forming H atoms and N(CH<sub>3</sub>)<sub>2</sub> species. While the N(CH<sub>3</sub>)<sub>2</sub> species bonds primarily to the adatoms, the H atoms can bond to either adatoms or restatoms. Possible reaction mechanism and the reactivity of the different types of surface silicon atoms are discussed.

© 2002 Published by Elsevier Science B.V.

*Keywords:* Silicon; Molecule–solid reactions; Chemisorption; Scanning tunneling microscopy; Photoelectron spectroscopy

## 1. Introduction

The Si(1 1 1)-(7 × 7) surface has been studied widely because its complex structure provides a rich variety of chemically inequivalent silicon atoms, leading to unusually complex and interesting chemistry. The dimer-adatom-stacking fault (DAS) model, first proposed by Takayanagi et al. [1], since confirmed by numerous other studies

[2–7], is depicted in Fig. 1. The primary structural features are (1) 12 adatoms forming a layer above the bulk-terminated (1 1 1) lattice, (2) a set of six “restatoms”, (3) a stacking fault under one-half of the unit cell, and (4) formation of dimers at the boundaries between the unit cells, and (5) a deep “corner hole” at the intersection of six unit cells. It is well-understood that the principal driving force for this complex reconstruction is the minimization of the number of Si atoms with coordination number less than 4 [1,8]. While the surface reconstruction achieves 4-fold coordination for the vast majority of Si atoms, the chemistry of the surface is dominated by the dangling bonds that remain on

\* Corresponding author. Tel.: +1-608-262-6371; fax: +1-608-262-0453.

E-mail address: [rjhamers@facstaff.wisc.edu](mailto:rjhamers@facstaff.wisc.edu) (R.J. Hamers).

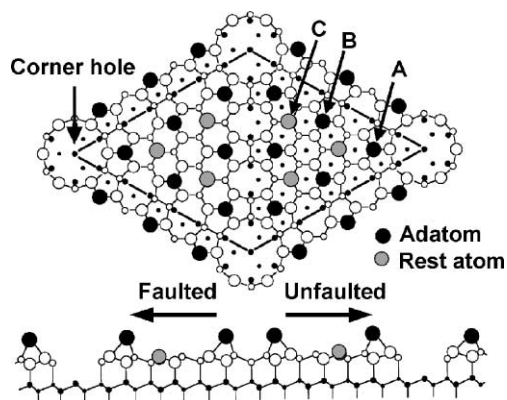


Fig. 1. Schematic diagram for Si(111)-(7 × 7) “DAS” model [1]. Corner adatoms (labeled A), center adatoms (labeled B), restatoms (labeled C) are identified by arrows.

the 19 atoms per unit cell that remain 3-fold coordinated: 12 on the adatoms, six on the restatoms, and one at the corner hole. The surface reconstruction is also accompanied by a variety of charge transfer processes. Consequently, the electron density is higher in the “faulted” than in the “unfaulted” half, and within each half the three adatoms nearest the corner hole (referred to as “corner adatoms”, labeled A in Fig. 1) are different from the remaining three (referred to as “center adatoms”, labeled B in Fig. 1) [5,6]. The six restatoms are labeled C in Fig. 1.

The chemistry of N-containing molecules is usually controlled by charge transfer processes involving the “lone pair” electrons on the nitrogen atom. Similar processes are also believed to control reactions on silicon surfaces [9–12]. A recent study [12] showed that on the Si(001) surface, trimethylamine (TMA) can form a surprisingly stable dative-bonded molecular adduct in which the N atom donates substantial electron density to the underlying Si atom, leaving the N atom in a quaternary, highly ionic environment. Similar experiments with dimethylamine (DMA), however, showed that dissociation occurs readily via cleavage of the N–H bond. Computational studies have shown that the ability to form stable dative-bonded adducts is closely connected with the ability to transfer charge from one silicon atom to another [12,13]. Since the reconstruction of the Si(111)-(7 × 7) surface also involves substantial

charge transfer between different atoms, a study of the interaction between simple amines and the Si(111)-(7 × 7) surface provides further insight into how these charge transfer processes impact the resulting surface chemistry.

## 2. Experiment

The experiments described here were performed in several different ultrahigh vacuum (UHV) chambers, each having base pressure of  $<1 \times 10^{-10}$  Torr. The Si(111) samples (0.005  $\Omega$  cm, As-doped) were rinsed in methanol and then cleaned of residual carbon contamination by exposure to ozone for approximately 15 min. The samples were degassed at  $\sim 850$  K overnight in the chamber and then annealed to 1400 K to remove the oxide layer. This procedure produces clean, well-ordered surfaces exhibiting the (7 × 7) reconstruction [14].

Direct observation of adsorbed molecules was achieved using a home-built UHV scanning tunneling microscope (STM). Images were obtained at sample bias voltage range from +1.2 to –3.0 V, utilizing a tunneling current of 100 pA.

X-ray photoelectron spectroscopy (XPS) were obtained using a Physical Electronics hemispherical analyzer and a monochromatized Al  $K_{\alpha}$  source (1486.6 eV). The Si(2p) peaks were used as an internal standard for both energy and intensity. The XPS spectra reported here have been adjusted to yield a constant 99.4 eV binding energy for the bulk Si(2p<sub>3/2</sub>) line. Peak widths are reported as the full-width at half-maximum (FWHM). Ultraviolet photoemission spectroscopy (UPS) experiments were performed in the same system, using a differentially pumped Vacuum Generators He I discharge source (21.2 eV). Spectra were obtained with a pass energy of 2.95 eV. To maximize the surface sensitivity, the UPS spectra were obtained with the analyzer at an angle of 80° from the surface normal. The Fermi level was determined by measuring the UPS spectrum for the tantalum clip on the sample holder. Sample temperatures were measured using an infrared pyrometer (for  $T > 750$  K) and by measuring the power applied to the sample during the experiment, and later cali-

brating with an thermocouple attached directly to the sample surface (for  $T < 750$  K); estimated accuracy is 50 K.

TMA and DMA were purchased from Aldrich with 99% purity. They were further purified through several freeze-pump-thaw cycles. The molecules were introduced to the UHV chambers through variable leak valves; in each vacuum system the purity of the introduced gases was verified in situ via mass spectroscopy. While the rise in chamber background pressure was used as an indicator for overall dose, the actual exposures at the surface are higher due to the chamber geometry. All exposures are given in Langmuirs (1 Langmuir  $\equiv 1 \text{ L} \equiv 1 \times 10^{-6}$  Torr s).

### 3. Results

#### 3.1. Trimethylamine on Si(111)

##### 3.1.1. Scanning tunneling microscopy

Fig. 2 shows constant-current STM images (100 pA tunneling current) of a clean Si(111)-(7 × 7) sample and the same sample after exposure to 0.1 L TMA at 300 K. The image for the clean surface (Fig. 2a) obtained with the sample biased at +1.6 V clearly shows the 12 adatoms of the (7 × 7) reconstruction in one unit cell. After the sample was exposed to 0.1 L TMA, STM images obtained with the sample biased at +1.2 V (Fig. 2b), reveal a large number of apparent protrusions (imaged as bright regions in the topographic images). Analysis of the spatial distribution of these protrusions shows that they are maximized directly above the known positions of the adatoms, with an apparent height approximately 2 Å higher than the surrounding adatoms.

Analysis of the spatial distribution of the protrusions shows that there is no detectable difference in the number of features in faulted vs. unfaulted subunits of the (7 × 7) unit cell. However, there is a significant preference for bonding at the center adatom sites compared to the corner adatoms sites. In Fig. 2b, for example, there are 25 bright protrusions (~83% of the total) bonded at center adatom sites and only 5 (~17%) at corner adatom sites. Similar analysis of other images

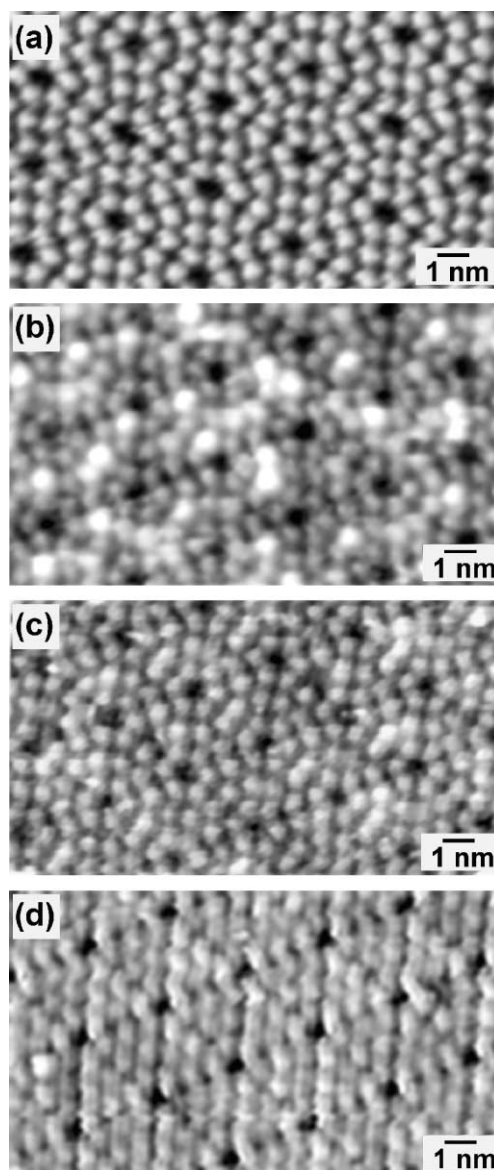


Fig. 2. STM images of a clean Si(111) surface and after exposed to 0.1 L TMA with a tunneling current of 100 pA and different sample biases. (a) The clean surface, +1.6 V, (b) after exposure, +1.2 V (c) after exposure, +1.0 V (d) after exposure, -1.6 V.

leads us to conclude that there is a persistent preference for bonding at the center adatom sites.

To help understand the nature of the molecular contrast obtained in the STM, images were obtained at other voltages. Fig. 2c shows that when

the sample bias is decreased to +1.0 V the adatoms of the  $(7 \times 7)$  reconstruction are still visible, but no distinct molecular features are observed. Similarly, when the sample bias is changed to negative values (thereby involving electrons tunneling out of occupied electronic states of the sample), the surface again appears nearly identical to the clean Si(111)- $(7 \times 7)$  surface over the entire bias range between  $-1.6$  (Fig. 2d) and  $-3.0$  V (not shown). Overall, we find that while positive bias voltages  $>1$  V lead to the observation of molecular features like those observed in Fig. 2b. At bias voltages between  $+1.0$  and  $-3.0$  V the molecular features are much more difficult to distinguish from the unreacted surface.

### 3.1.2. X-ray photoelectron spectroscopy data

In order to identify the chemical species observed in STM images, XPS experiments were performed. Fig. 3 shows N(1s) and C(1s) spectra of a Si(111) surface after exposure to different doses of TMA at 300 K. After 0.5 L exposure, the N(1s) spectrum shows one dominant peak at 402.4 eV with a FWHM of 1.0 eV. The C(1s) spectrum likewise shows a dominant peak at 287.5 eV with a FWHM of 0.9 eV, close to the resolution of the XPS instrument. Higher exposure leads to the formation of additional surface species giving rise to a small N(1s) peak at 399.1 eV and weaker C(1s) peaks at 284.5–286.4 eV. After exposures higher than 20 L, the higher binding energy peak remains nearly unchanged, but the peaks at lower binding energy increase significantly in intensity and at an exposure of 80 L, represent the dominant contribution to the total spectrum. Overall, the C(1s) and N(1s) spectra show that adsorption initially forms the N(1s) and C(1s) peaks at high binding energy, which saturate after  $\sim 20$  L exposure. Further exposure occurs with a lower reaction probability and preferentially yields the peaks with lower binding energy.

Although the surface never achieves a true “saturation” coverage, we note that the initial adduct saturates at exposures of  $\sim 20$  L, and that at this coverage the high-binding energy peaks represent  $\sim 80\%$  of the total N(1s) and C(1s) area. Quantitative analysis of peak areas shows that after exposing a Si(111)- $(7 \times 7)$  surface to 20 L

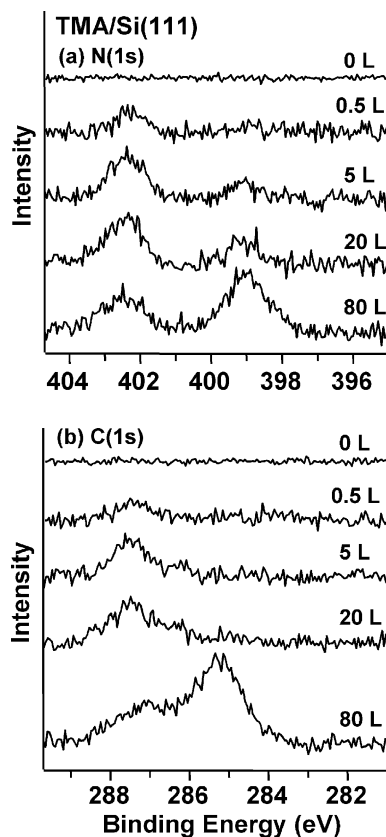


Fig. 3. (a) N(1s) and (b) C(1s) XPS spectra of a Si(111) surface exposed to different doses of TMA at 300 K.

TMA, the ratio of total N(1s) to Si(2p) peak areas ( $A_{N1s}/A_{Si2p}$ ) is 0.8. For comparison, we also measured the corresponding spectra (not shown) after saturation exposure of a Si(001) surface to ammonia ( $NH_3$ ) and to TMA, under identical experimental conditions. The adsorption of ammonia on Si(001) yielded a single N(1s) peak at 399.1 eV and an area ratio  $A_{N1s}/A_{Si2p}$  of 3.4 for a saturated surface [12]. Similarly, the adsorption of TMA on Si(001) yielded spectra similar to those observed here on the (111) surface, but with an area ratio  $A_{N1s}/A_{Si2p}$  of 1.6. Since previous studies have established that the saturation N coverage for  $NH_3/Si(001)$  is about 1 nitrogen atom per 2 silicon atoms ( $\sim 3.3 \times 10^{14} \text{ cm}^{-2}$ ) [15] we can estimate the N coverage from 20 L TMA on Si(111) to be approximately six nitrogen atoms per  $(7 \times 7)$  unit cell.

Quantitative analysis of the N(1s) spectra shows that although the initial adduct saturates after  $\sim 20$  L exposure, the total N coverage continues to increase slowly at higher exposures. After exposure to 80 L, the N coverage (now consisting primarily of the low-binding energy peaks) corresponds to  $\sim 12$  nitrogen atoms per unit cell. An experiment at a much higher exposure ( $\sim 200$  L) on a 190 K surface (spectrum not shown) yielded peaks at the same energies, with an N coverage of  $\sim 23$  nitrogen atoms per unit cell. At exposures of  $>20$  L the N(1s) and C(1s) peak areas increase only slowly with exposure; this indicates that the sticking probability is smaller than what is observed at lower exposures.

Fig. 4 shows the results of a thermal stability study in which a Si(1 1 1) sample was exposed to 20 L of TMA at 300 K, then was heated for 10 min to

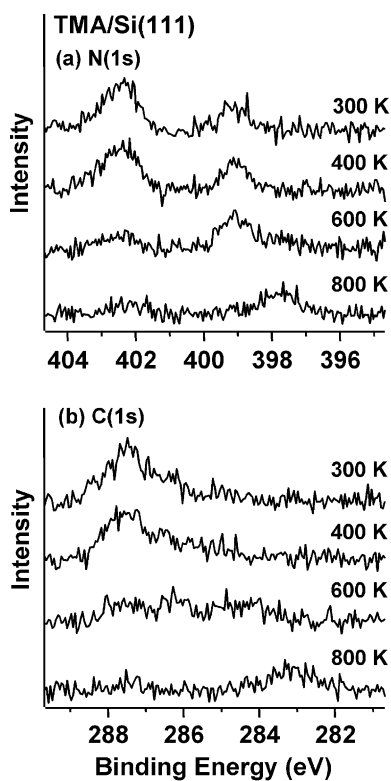


Fig. 4. (a) N(1s) and (b) C(1s) XPS spectra of a Si(1 1 1) surface exposed to 20 L of TMA at 300 K and subsequently annealed at elevated temperature. All spectra were obtained after cooling the sample back to 300 K.

the temperatures indicated in the figure, and finally was cooled to 300 K for XPS analysis. Annealing to 400 K induces a decrease in the area of the N(1s) peak at 402.4 eV and the C(1s) peak at 287.5 eV, with a corresponding increase in the area of the N(1s) peak at 399.1 eV and the C(1s) peaks at 284.5–286.4 eV. Since the total C(1s) and N(1s) peak areas do not change, we conclude that heating to 400 K induces some dissociation, but without any significant desorption. However, annealing to 600 K significantly decreases the intensities of the 402.4 eV N(1s) peak and the 287.5 eV C(1s) peak and also causes a  $\sim 40\%$  decrease in the total peak area, suggesting that some species desorb from the surface. Further annealing to 800 K leads to a N(1s) peak at 397.7 eV and a C(1s) peak at 283.2 eV, which arise from silicon nitride and silicon carbide, respectively [16–20].

The XPS spectra in Figs. 3 and 4 include N(1s) and C(1s) peaks at quite high binding energies. The 402.4 eV N(1s) binding energy is much higher than the values of 398.5–399.5 eV observed for typical amines [11,16,21–24] and is close to the value of 402.2 eV we observed previously for TMA on the Si(00 1) surface. It also approaches the value of 403.2 eV we obtained for the ionic salt ammonium chloride [12] as well as the literature value of 402.5 eV for  $(\text{CH}_3)_4\text{NCl}$  [25]. These data indicate that the N(1s) peak at 402.4 eV for TMA/Si(1 1 1) corresponds to a highly ionic, dative-bonded adduct in which the N atom interacts with the surface by donating electron density to the Si surfaces. This electron donation leaves the N atom with a coordination number of 4 and a formal charge of +1, much like the ammonium ion. We attribute the smaller XPS peak at 399.1 eV, which is identical to the feature observed for adsorption of DMA that will be discussed below, to  $\text{Si-N}(\text{CH}_3)_2$  fragments produced via cleavage of N–C bonds. This assignment is also supported by the fact that heating decreases the 402.4 eV peak and increases the 399.1 eV peak.

### 3.1.3. Ultraviolet photoemission data

UPS experiments were performed to determine which electronic states of the surface are involved in the chemisorption process. Fig. 5 shows UPS spectra of a clean Si(1 1 1) surface, and the same

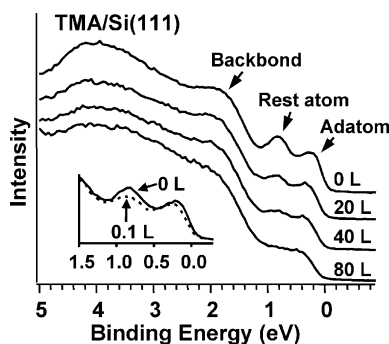


Fig. 5. UPS spectra of a clean Si(111) surface and after exposure to TMA at different exposures.

surface after exposure to increasing amounts of TMA. The spectrum of the clean surface clearly shows two surface states at 0.2 and 0.8 eV, which correspond to the adatom state and restatom state, respectively [5,26]. Additionally, a small peak is observed at 1.8 eV, that has been attributed previously to the backbonds between the Si adatoms and the outermost bulk-like Si(111) layer [20]. After a nominal exposure of 0.1 L, the peaks associated with the adatom and restatom states both decrease in intensity. The adatom state also shifts toward higher binding energy, while the restatom state remains unchanged. Although quantitative analysis is difficult due to emission from the bulk states, it appears that the restatom state near 0.8 eV decreases more quickly than the adatom state. However, even at an exposure of 80 L, the surface-state emission is not quenched entirely, and substantial emission at 0.2–0.9 eV remains. We also note that the peak associated with the adatom backbond state decreases in intensity after 80 L exposure. A further experiment on a cold (190 K) sample exposed to  $\sim 200$  L TMA showed quenching of virtually all intensity associated with the adatom, restatom, and backbond states.

### 3.2. Dimethylamine on Si(111)

DMA exhibits behavior quite different from that of TMA. Fig. 6 shows N(1s) and C(1s) XPS spectra of a Si(111) sample exposed to 10 L of DMA at 300 K. The N(1s) spectrum is characterized by a large, narrow (1.0 eV FWHM) peak at

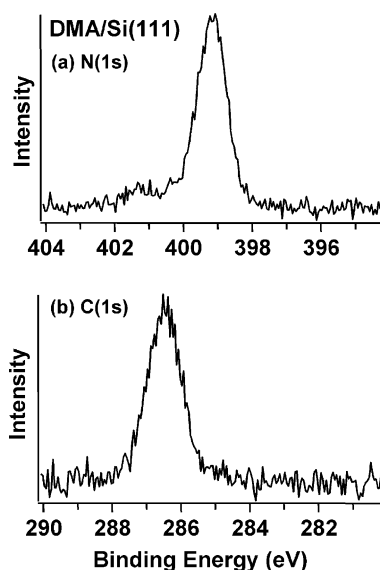


Fig. 6. (a) N(1s) and (b) C(1s) XPS spectra of a Si(111) surface exposed to 10 L of DMA at 300 K.

399.1 eV, with a tiny additional peak near 401.2 eV. The C(1s) spectrum is well-described by single peak at 286.4 eV with a width of a FWHM of 1.2 eV, which is slightly broader than the instrumental linewidth. The 399.1 eV binding energy of the major N(1s) peak is close to the 398.5–399.1 eV N(1s) binding energies of dissociatively adsorbed ammonia [16,21,22], pyrrolidine [11], aniline [11,23], and DMA [12] on Si(001) surfaces. In all these compounds adsorption occurs via cleavage of an N–H bond, leaving the N atom with a coordination number of three. Thus, we conclude that the 399.1 eV peak we observe here also arises from DMA molecule in which the N atom has a coordination number of three. Since there is little difference in electronegativity between H and C, it cannot be readily determined from the N(1s) data alone whether DMA cleaves N–H or N–C bonds when adsorbing to the Si(111) surface. However, cleavage of an N–C bond would be expected to produce methyl fragments bonded to the silicon surface (i.e., Si–CH<sub>3</sub> species). In a previous study, we found that Si–CH<sub>3</sub> species on the Si(001) surface yielded a C(1s) binding energy 284.1 eV [12]. In contrast, the C(1s) spectrum for DMA on Si(111) primarily shows a single peak with a

binding energy of 286.4 eV, more than 2 eV higher than that of the Si–CH<sub>3</sub> species. Thus, the absence of any significant intensity at 284.1 eV indicates that there is no significant cleavage of N–C bonds, and leads us to conclude that DMA bonds to the Si(111) surface by cleaving the N–H bond, leaving N(CH<sub>3</sub>)<sub>2</sub> species and H atoms on the surface. This behavior is very similar to that observed previously on the Si(001) surface [12].

Quantitative analysis of the XPS data for DMA/Si(111) yields an  $A_{N1s}/A_{Si2p}$  ratio of 1.35. This area ratio is significantly higher than the value of 0.78 observed from a Si(111)-(7 × 7) surface exposed to TMA, but is again much lower than the value of 2.51 obtained for a Si(001) exposed to DMA under the same experimental conditions and with the same exposure [27]. Thus, we conclude that the Si(111)-(7 × 7) surface is able to adsorb more DMA molecules than TMA molecules. Again using NH<sub>3</sub>/Si(001) as a calibration, we conclude that the saturation coverage of DMA on Si(111) corresponds to ~10 nitrogen atoms per (7 × 7) unit cell.

To facilitate determination of the surface sites involved in bonding to DMA, STM images were obtained of Si(111)-(7 × 7) surfaces exposed to DMA. Fig. 7 shows an image (sample bias –1.6 V, tunneling current 100 pA) obtained after a nominal exposure of 0.01 L DMA. The (7 × 7) unit cells of the surface reconstruction are clearly seen; however, exposure to DMA induces two types of new features, labeled “A” and “B”. The “A” features each consist of a round protrusion that has a local maximum located directly on top of an adatom, approximately 2 Å higher than the surrounding surface. Each “B” feature also appears as a local protrusion centered on an adatom site, but with its local maximum ~1 Å below the height of the unreacted adatoms. Both features are observed more frequently on center adatoms than on corner adatoms.

More information about how different surface states are involved in the reaction is provided by UPS. Fig. 8 shows UPS spectra of a clean Si(111) surface, and also the same surface after exposure to DMA. Before exposure the adatom and restatom states are clearly visible with binding energies 0.2 and 0.8 eV, respectively, and the backbond

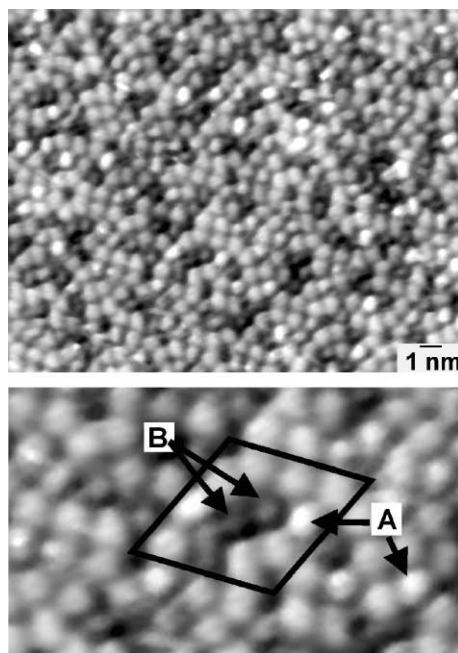


Fig. 7. The STM image of a Si(111) surface exposed to 0.01 L DMA with a tunneling current of 100 pA and a sample bias of –1.6 V.

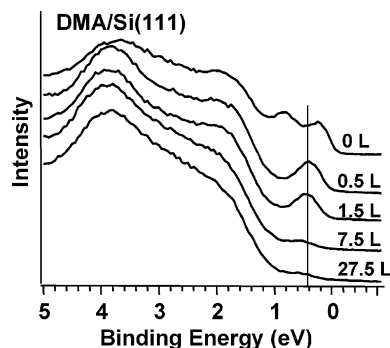


Fig. 8. UPS spectra of a clean Si(111) surface and after exposure to DMA at different exposures.

state can be observed as a smaller peak at 1.8 eV binding energy. After 0.5 L most of the intensity from the restatom state is quenched. The adatom states also decreases in intensity and shows a small increase in binding energy from 0.2 to 0.4 eV, while the backbond state remains clearly visible. At high exposures (7.5 and 27.5 L), the adatom state and the backbond state near 2.0 eV both appear to be quenched.

## 4. Discussion

### 4.1. Interaction of TMA with Si(111)

The XPS results show that at low exposures ( $\leq 0.5$  L), TMA adsorbs to the Si(111) surface primarily in a molecular form, via formation of a dative bond. From the new information provided by STM and UPS, it is possible to develop a more comprehensive understanding of how TMA interacts with the valence electronic states.

Since the STM images also show only one type of feature, we conclude that the bright protrusions observed in the STM images in Fig. 2b correspond to intact TMA molecules. Thus, the STM images support the conclusion that the TMA molecules primarily interact with the adatoms. Closer inspection of the STM images reveals that  $\sim 83\%$  of the TMA molecule react with the center adatoms, and only  $\sim 17\%$  react with the corner adatoms. Thus, we find that the center adatoms are significantly more reactive than the corner adatoms.

The greater propensity for bonding at the adatoms compared with the restatoms can be explained on the basis of the charge density on each of the different types of atoms exposed at the Si(111)-(7  $\times$  7) surface. Formation of the Si(111)-(7  $\times$  7) unit cell leads to 19 Si atoms per unit cell that have only 3-fold coordination. Twelve of these dangling bonds are located on the adatoms, six on the restatoms, and one at the corner of the unit cell, in the deep hole extending down to the next layer. Photoemission and tunneling spectroscopy studies have shown that the “restatom” and “corner hole” states are fully occupied, leaving only five electrons to distribute among the 12 adatoms [28]. Thus, the average charge on the adatoms is approximately  $+7/12$ . This basic picture is also verified through high-resolution core-level photoemission measurements showing that adatoms yield a Si(2p) binding energy 0.53 eV higher than that of the bulk atoms, while the restatoms yield a binding energy 0.7 eV lower than that of the bulk atoms [29,30]. These difference in binding energy indicate that the adatoms are positively charged and the restatoms are negatively charged. First-principles theoretical calculations also show similar behavior [31,32]. Thus, it appears that the

positively charged adatoms can more readily act as electron acceptors compared with the negatively charged restatoms.

The greater propensity for bonding at the center adatoms compared with the corner adatoms can be understood on the basis of the more subtle differences between the different types of adatoms. STM images and tunneling spectroscopy measurements obtained at small negative bias show that the center adatoms appear lower than the corner adatoms [6,8]. These differences in apparent height indicate that the density of filled valence states near the Fermi energy is lower on the center adatoms than on the corner adatoms [6,8,33]. Indeed, first-principles electronic structure calculations also show that corner adatoms retain more of their electron density than do the center adatoms [32]. These observations are easily justified by simple geometric reasoning: since the center adatoms are adjacent to two restatoms while the corner adatoms are adjacent to only one, the center adatoms can more readily donate electron density to the restatoms. Thus, the center adatoms retain less electron density and are consequently more positively charged than the corner adatoms are. Since dative bond formation involves donation of electrons from the N atom “lone pair” to the Si surface, the most positively charged atoms are expected to more readily act as electron acceptors. Although the electron density in the “faulted” half is predicted to be higher than that in the “unfaulted” half of each Si(111)-(7  $\times$  7) unit cell [32], our experiments do not show any significant difference in reactivity between the two halves.

The above picture explains the intrinsic reactivity of the adatoms and the higher reactivity of center adatoms compared with “corner” adatoms at low coverages. Surprisingly, however, the UPS data (Fig. 5) show that the restatom state at 0.8 eV is also affected even after only 0.1 L exposure of TMA. The apparent involvement of restatoms can be attributed to two factors. First, since formation of the (7  $\times$  7) reconstruction involves transfer of electron density from the adatoms to the restatoms, formation of a bond (either a dative bond or a more conventional, covalent bond) at the adatom may alter this charge transfer and thereby

affect both the adatom and restatom surface states. A second contributing factor may be dissociation induced by the ultraviolet lamp used for UPS experiments. A test in which we obtained XPS spectra before and after exposing a 0.1 L-exposed Si(111) surface to UV light from the UPS He discharge lamp for 5 min (the typical illumination time for acquisition of a complete spectrum) showed that at these low coverages, the UPS source could be responsible for dissociation of  $\sim 40\%$  of the TMA molecules.

At high exposures ( $\geq 80$  L), the XPS data provides clear evidence for dissociation of TMA. The predominant N(1s) and C(1s) peaks arise at energies identical to where Si–N(CH<sub>3</sub>)<sub>2</sub> dissociation fragments have been observed on the Si(001) surface [12]. While dissociation likely involves the adatoms, at these high coverages quantitative analysis of the XPS data suggests that the reaction may involve multiple surface sites. At high exposures, the UPS data also shows the elimination of the backbond state at 1.8 eV. The disappearance of this state suggests that at least some of the molecules react via insertion between the adatoms and the underlying bulk-like Si(111) layer. Previous studies have suggested a similar reaction between ammonia molecules and adatom backbonds [20,34].

The bias-dependence of STM images also provides us further insight into the electronic properties of the TMA-adsorbed Si(111) surface. At sample voltages between  $-1.6$  and  $-3.0$  V (thereby involving occupied electronic states of the sample), surface appears very much like the clean surface, and no features that can be attributed to adsorbed molecules are observed. This indicates that the highest-occupied molecular orbital of the TMA fragment lies more than 3 eV below the Fermi level. The molecular features begin to appear at a positive bias of  $+1.2$  V, suggesting the LUMO orbitals of the adsorbed TMA lie at  $\sim 1.2$  eV above the Fermi level.

#### 4.2. Interaction of DMA with Si(111)

While TMA can bond to the Si(111) surface molecularly through a dative-bonded configuration, the XPS data show that DMA bonds disso-

ciatively by breaking the N–H bond to form Si–N(CH<sub>3</sub>)<sub>2</sub> and Si–H species. This behavior is very similar to that observed on the Si(001) surface [12]. Again, however, the more complex structure of the Si(111)-(7 × 7) surface leads to preferential reaction at specific sites. Previous STM studies have shown that under the imaging conditions used here the adatoms that have a H atom bonded to them appear lower (darker) than unreacted adatoms [35,36]. Thus, we conclude that the darker adatoms (feature B in Fig. 7) arise from the adatoms with an H atom bonded to them, and the bright protrusions (feature A) arise from the N(CH<sub>3</sub>)<sub>2</sub> species. Analysis of the distribution of reacted atoms shows that the N(CH<sub>3</sub>)<sub>2</sub> species are more frequently bonded to center adatom sites than to corner adatom sites. Since TMA also showed preferential bonding at the center adatom sites, the STM data suggests that the DMA molecules may likewise form a dative-bonded adduct, followed by N–H bond cleavage. The strong preference for N–H compared with N–C bond cleavage has been explored previously and shown to arise from the fact that withdrawal of electron density from the N atom (from dative bond formation) leads to a lowering of the barrier for N–H cleavage, while for N–C cleavage a significant barrier remains [12]. A similar result has been observed more generally for organic amines: although N–C bond cleavage may lead to more favorable end products, the barrier to N–H bond cleavage is lower and therefore occurs more readily [37–39].

While it is very likely that the Si–N(CH<sub>3</sub>)<sub>2</sub> species are at the adatom sites, the H atoms produced by dissociation can in principle be located on either adatom or restatom sites. While we clearly observe some H atoms on adatom sites via STM, identification of any species bonded to the restatoms sites is difficult with STM since these atoms are located one full atomic layer below the adatoms. However, the UPS data clearly show that upon DMA exposure the surface state associated with the filled dangling bond of the restatoms decreases in intensity even more quickly than does the adatom state. There may be several factors contributing to this decrease. As noted above, bond formation to the adatoms also

modifies the charge transfer to the restatoms and would be expected to affect the restatom state, in a manner similar to that proposed previously for ammonia [40–42]. A second contributing factor is that there are only half as many restatoms (six per unit cell) as adatoms (12 per unit cell). If (for example) each DMA molecule dissociated to produce one fragment on an adatom and another fragment on a restatom, then at higher coverage one would expect the six restatom states to be completely quenched when only half the adatoms have reacted. Thus, based on the STM and UPS data, it is likely that H atoms can bond to both adatoms and restatoms.

It is quite intriguing that upon DMA exposure the adatom state exhibits an apparent shift in binding energy from 0.2 to 0.4 eV. A recent high-resolution UPS study of the Si(1 1 1)-(7 × 7) surfaces at low temperature clearly observed two adatom states: one at 0.15 eV below the Fermi level that was attributed to the center adatoms, and a second at 0.5 eV below the Fermi level that was attributed to the corner adatoms [43]. Since our STM data indicates that the center adatoms react first, the ~0.2 eV shift we observe in Fig. 8 is completely consistent with this assignment.

Overall, then, the picture that emerges from the STM and photoemission data is that that DMA first interacts preferentially with the center adatoms, via a dative-bonded intermediate. The increased positive charge on the N atom leads to rapid dissociation via cleavage of an N–H bond. The Si–N(CH<sub>3</sub>)<sub>2</sub> products remain on the adatom sites, and the H atoms are distributed among the restatoms and the adatoms. After the same exposures, the coverage of DMA is much lower on the Si(1 1 1)-(7 × 7) surface than on the Si(0 0 1) surface for two reasons: (1) because the reaction of the first molecules alters the adatom-to-restatom charge transfer, thereby making the remaining adatoms less able to act as electron acceptors for the dative-bonded intermediate, and (2) because dissociation of dative-bonded DMA molecules is inhibited by the absence of nearby sites for the H atom to bond. However, comparing with TMA, DMA react with Si(1 1 1) more efficiently.

## 5. Conclusions

Our results show that reactions of amines with silicon surfaces can be understood on the basis of charge transfer between the N atom “lone pair” and the Si surface. We showed previously that on the Si(0 0 1) surface, dative bond formation involved electron donation from the N atom lone pair to a Si atom, which was facilitated by the ability to delocalize this charge onto the adjacent Si atom [12]. Here, we show that on the Si(1 1 1)-(7 × 7) surface, the presence of various surface sites with varying charge densities likewise leads to spatially selective reaction chemistry of TMA. The center adatoms of the (7 × 7) reconstruction exhibit the highest propensity for dative bond formation, which can be attributed to the fact that these are also the most electron-deficient atoms accessible for reaction with the TMA molecules. Overall, this work, together with prior work on the Si(0 0 1) surface, demonstrates that silicon surfaces can act as excellent electron acceptors, and that the chemistry of amines and other electron-rich molecules can be understood largely on the basis of the local charge density and the ability to transfer charge between different Si atoms. Even though reactions such as adsorption of DMA ultimately result in bonds that are primarily covalent in nature, highly ionic species like those observed for TMA may play critical roles in controlling the mechanistic pathways.

## Acknowledgements

This work was supported by National Science Foundation, CHE-0071385. The authors gratefully acknowledge Michael Schwartz for his assistance with the STM instrument.

## References

- [1] K. Takayanagi, Y. Tanishiro, M. Takahashi, S. Takahashi, *J. Vac. Sci. Tech. A* 3 (1985) 1502–1506.
- [2] R.M. Tromp, *Surf. Sci.* 155 (1985) 432.
- [3] I.K. Robinson, W.K. Waskiewicz, P.H. Fuoss, J.B. Stark, P.A. Bennett, *Phys. Rev. B* 33 (1986) 7013–7016.
- [4] J.E. Northrup, *Phys. Rev. Lett.* 57 (1986) 147–154.

- [5] R.J. Hamers, R.M. Tromp, J.E. Demuth, *Phys. Rev. Lett.* 56 (1986) 1972–1975.
- [6] R.J. Hamers, R.M. Tromp, J.E. Demuth, *Surf. Sci.* 181 (1987) 246–355.
- [7] S. Ihara, T. Uda, M. Hirao, *Appl. Surf. Sci.* 60-1 (1992) 22–28.
- [8] R.M. Tromp, R.J. Hamers, J.E. Demuth, *Science* 324 (1986) 304.
- [9] E. Fattal, M.R. Radeke, G. Reynolds, E.A. Carter, *J. Phys. Chem. B* 101 (1997) 8658–8661.
- [10] Y. Widjaja, M.M. Mysinger, C.B. Musgrave, *J. Phys. Chem. B* 104 (2000) 2527–2533.
- [11] X. Cao, S.K. Coulter, M.D. Ellison, H. Liu, J. Liu, R.J. Hamers, *J. Phys. Chem. B* 105 (2001) 3759–3768.
- [12] X. Cao, R.J. Hamers, *J. Am. Chem. Soc.* 123 (2001) 10988–10996.
- [13] C. Mui, G.T. Wang, S.F. Bent, C.B. Musgrave, *J. Chem. Phys.* 114 (2001) 10170–10180.
- [14] R.J. Hamers, R.M. Tromp, J.E. Demuth, *Phys. Rev. B* 34 (1986) 5343–5357.
- [15] P.A. Taylor, R.M. Wallace, W.J. Choyke, M.J. Dresser, J.T. Yates Jr., *Surf. Sci.* 215 (1989) L286–L292.
- [16] C.H.F. Peden, J.W. Rogers Jr., N.D. Shinn, K.B. Kidd, K.L. Tsang, *Phys. Rev. B* 47 (1993) 15622–15629.
- [17] J.F. Moulder, W.F. Stickle, P.E. Sobol, K.D. Bomben, *Handbook of X-ray photoelectron spectroscopy*, Perkin-Elmer Corporation, Eden Prairie, 1992.
- [18] W.F. Bergerson, M.A. Mulder, R.P. Hsung, X.Y. Zhu, *J. Am. Chem. Soc.* 121 (1999) 454–455.
- [19] F. Bozso, P. Avouris, *Phys. Rev. B* 38 (1988) 3937–3942.
- [20] M. Björkqvist, M. Göthelid, T.M. Grehk, U.O. Karlsson, *Phys. Rev. B* 57 (1998) 2327–2333.
- [21] J.L. Bischoff, F. Lutz, D. Bolmont, L. Kubler, *Surf. Sci.* 251/252 (1991) 170–174.
- [22] G. Dufour, F. Rochet, H. Roulet, F. Sirotti, *Surf. Sci.* 304 (1994) 33–47.
- [23] T. Kugler, U. Thibaut, M. Abraham, G. Folkers, W. Gopel, *Surf. Sci.* 260 (1992) 64–74.
- [24] X.-Y. Zhu, J.A. Mulder, W.F. Bergerson, *Langmuir* 15 (1999) 8147–8154.
- [25] B.J. Lindberg, J. Hedman, *Chemica Scripta* 7 (1975) 155–166.
- [26] G.V. Hansson, R.I.G. Uhrberg, *Surf. Sci. Rep.* 9 (1988) 197–292.
- [27] X. Cao, R.J. Hamers, *J. Vac. Sci. Technol. B* 20 (2002) 1614–1619.
- [28] J.E. Northrup, *Phys. Rev. Lett.* 57 (1986) 154–157.
- [29] C.J. Karlsson, E. Landemark, Y.-C. Chao, R.I.G. Uhrberg, *Phys. Rev. B* 50 (1994) 5767–5770.
- [30] J.J. Paggel, W. Theis, K. Horn, C. Jung, C. Hellwig, H. Petersen, *Phys. Rev. B* 50 (1994) 18686–19689.
- [31] G.X. Qian, D.J. Chadi, *Phys. Rev. B* 35 (1987) 1288–1293.
- [32] I. Stich, M.C. Payne, R.D. King-Smith, J.S. Lin, L.J. Clarke, *Phys. Rev. Lett.* 68 (1992) 1351–1354.
- [33] J. Tersoff, D.R. Hamann, *Phys. Rev. B* 31 (1985) 805–813.
- [34] H. Ezzehar, P. Sonnet, C. Minot, L. Stauffer, *Surf. Sci.* 454-456 (2000) 358–362.
- [35] K. Mortensen, D.M. Chen, P.J. Bedrossian, J.A. Golovchenko, F. Besenbacher, *Phys. Rev. B* 43 (1991) 1816–1819.
- [36] J.J. Boland, *Surf. Sci.* 244 (1991) 1–14.
- [37] A.I. Boldyrev, J. Simons, *J. Chem. Phys.* 97 (1992) 6621–6627.
- [38] S.A. Shaffer, F. Turecek, *J. Am. Chem. Soc.* 116 (1994) 8647–8653.
- [39] S.A. Shaffer, M. Sadílek, F. Turecek, *J. Org. Chem.* 61 (1996) 5234–5245.
- [40] R. Wolkow, P. Avouris, *Phys. Rev. Lett.* 60 (1988) 1049–1052.
- [41] P. Avouris, R. Wolkow, *Phys. Rev. B* 39 (1989) 5091–5100.
- [42] P. Avouris, F. Bozso, *J. Phys. Chem. B* 94 (1990) 2243–2245.
- [43] R.I.G. Uhrberg, T. Kaurila, Y.-C. Chao, *Phys. Rev. B* 58 (1998) R1730–R1733.